Towards Integration of GLAS into a National Fuel Mapping Program

Birgit Peterson, Kurtis Nelson, and Bruce Wylie

Abstract

Comprehensive canopy structure and fuel data are critical for understanding and modeling wildland fire. The LANDFIRE project produces such data nationwide based on a collection of field observations, Landsat imagery, and other geospatial data. Where field data are not available, alternate strategies are being investigated. In this study, vegetation structure data available from GLAS were used to fill this data gap for the Yukon Flats Ecoregion of interior Alaska. The GLAS-derived structure and fuel layers and the original LANDFIRE layers were subsequently used as inputs into a fire behavior model to determine what effect the revised inputs would have on the model outputs. The outputs showed that inclusion of the GLAS data enabled better landscape-level characterization of vegetation structure and therefore enabled a broader wildland fire modeling capability. The results of this work underscore how GLAS data can be incorporated into LANDFIRE canopy structure and fuel mapping.

Introduction

Wildland fire has significant impacts on ecosystems and human populations. Accurate assessments of canopy fuel, among other parameters, are needed to understand fire behavior and predict fire occurrences. A major source of spatial canopy fuel data for the US is the LANDFIRE, or Landscape Fire and Resource Management Planning Tools, program, a collaborative effort of the US Department of Interior, US Forest Service, and other partners. LANDFIRE consists of over 20 geospatial layers (see *www.landfire.gov* for complete list and descriptions) and aspatial databases describing potential and existing vegetation type, existing vegetation structure, surface and canopy fuel, and fire regimes, including historical fire frequency and severity and vegetation departure from reference conditions (Rollins, 2009). LANDFIRE data products are mapped at a 30 m spatial resolution and continuous data coverage is provided for all 50 states.

LANDFIRE canopy fuel layers include estimates of forest canopy height (CH), forest canopy cover (CC), canopy base height (CBH) and canopy bulk density (CBD; Reeves *et al.*, 2009). CH is the average height of forested vegetation within a pixel. CC is the percentage of the ground obscured by forested vegetation. CBH is the lowest height within the canopy at which sufficient fuel exists to propagate fire vertically into the canopy, as determined by a threshold based on field observations (Reinhardt *et al.*, 2006). CBD is the mass of available canopy fuel per unit of canopy volume. These variables are used to represent the structure of canopy fuel in fire risk, fire behavior, and fire effects models.

Traditionally, fuel parameters are obtained through field observations of vegetation structure providing detailed tree-level inventory data. While providing accurate descriptions of fuel conditions, collecting such data is resource intensive and costly, especially for remote areas. Furthermore, reliance on disparate field data collections, using non-standardized protocols, complicates the production of nationally consistent maps. In contrast, remote sensing provides consistent, comprehensive data over large areas and can be easily integrated with other spatial data to create fuel maps. For example, Keane *et al.* (2000) derived the necessary layers for fire behavior modeling in the Gila National Forest, New Mexico using a combination of Landsat-5 Thematic Mapper (TM) imagery, field data, terrain modeling, and ancillary data. Rollins *et al.* (2004) combined field data, Landsat TM imagery, aerial photos, ecosystems simulation, and biophysical gradient modeling to map fuel and fire regimes in Montana. Falkowski *et al.* (2005) used Advanced Spaceborne Thermal Emission and Reflection Radiometer data and gradient modeling to produce spatial surface and canopy fuel inputs for fire behavior modeling in Idaho.

More recently, lidar has been used to quantify vegetation canopy structure (Dubayah and Drake, 2000; Lefsky *et al.*, 2002), and is particularly useful for mapping fuel (Andersen *et al.*, 2005; Erdody and Moskal, 2010; Morsdorf *et al.*, 2004; Popescu and Zhao, 2008; Riaño *et al.*, 2004; Vauhkonen, 2010). While these previous studies used airborne, discrete-return lidar data, recent work has shown the applicability of spaceborne Geoscience Laser Altimeter System (GLAS) large-footprint (nominally ~65 m diameter), waveform data for estimating forest canopy structure. Pang *et al.* (2008) compared estimates of observed crown area weighted height values from data collected at sites throughout the western US to GLAS-derived metrics. They achieved an R^2 of 0.69 with a root mean square error of 6.2 m. Nelson *et al.* (2009) estimated timber volume in Siberia using GLAS and Moderate Resolution Imaging Spectroradiometer data, with error bounds of ± 11.8 m^3/ha in low slope and ± 12.4 m^3/ha in high slope conditions. Sun *et al.* (2008) compared height indexes derived from the Laser Vegetation Imaging Sensor (LVIS) and GLAS, which have been shown to be correlated with canopy structure characteristics. For example, Drake *et al.* (2002) found that the 50th percentile height of cumulative energy (H50) was correlated with biomass. Sun *et al.* (2008) attained R^2 values of up to 0.77 between LVIS- and GLAS-derived H50 metrics.

Birgit Peterson is with ASRC Research and Technology Solutions, Contractor to United States Geological Survey (USGS) Earth Resources Observation and Science (EROS) Center, 47914 252nd Street, Sioux Falls, SD 57198 (bpeterson@usgs.gov).

Kurtis Nelson and Bruce Wylie are with the USGS EROS, 47914 252nd Street, Sioux Falls, SD 57198.

Photogrammetric Engineering & Remote Sensing
Vol. 79, No. 2, February 2013, pp. 175–183.

0099-1112/13/7902–175/$3.00/0

Data from airborne systems often enable very detailed, high-resolution descriptions of vegetation structure, however they are neither nationally consistent nor contiguous. In contrast, between 2003 and 2009, GLAS sampled data globally, though at discrete points along disparate tracks, with 172 m along-track spacing between footprint centers. Therefore, while the vegetation structure data obtained from the GLAS waveforms are consistent, they are not spatially continuous, requiring modeling between sampled points. This can be accomplished by integrating remotely sensed imagery and ancillary data layers with the GLAS data to model vegetation structure continuously over large areas.

While some vegetation structure and fuel parameters can be directly inferred from lidar data, others must be modeled, often using empirical approaches such as regression against metrics derived from field observations (Dubayah and Drake, 2000). The derivation of vegetation structure parameters from airborne lidar data, most notably canopy height, has become commonplace. The utility of GLAS data has also been successfully demonstrated for estimating canopy height in a variety of biomes (Lefsky *et al.*, 2007; Los *et al.*, 2011; Selkowitz *et al.*, 2012) and has also been used recently to estimate other fuel-related parameters (García *et al.*, 2012; Neuenschwander *et al.*, 2008). The results of these previous studies advance the investigation of large scale mapping initiatives utilizing vegetation structure estimates from lidar. This paper seeks to expand on previous work using lidar for estimating canopy fuel over large areas and integrating different lidar data sources.

Objective

The objective of this study is to demonstrate a method for deriving a consistent, nationally-available, three-dimensional vegetation structure dataset for informing high quality canopy fuel maps. Specifically, lidar data collected at different scales are leveraged to prototype regional-to-national scale canopy fuel mapping methods for a study area in interior Alaska. By linking canopy fuel parameters derived from airborne lidar data and GLAS, the utility of GLAS data for obtaining the desired vegetation structure characteristics is demonstrated. Finally, the impact of using lidar-derived canopy fuel data on wildland fire modeling results is highlighted by comparing simulated fire behavior using LANDFIRE and lidar-derived canopy fuel inputs.

Study Area

The study area is located in the Yukon Flats Ecoregion (YFE; Gallant *et al.*, 1995) of interior Alaska and encompasses approximately 33,400 km^2 (Figure 1). Much of the vegetation is comprised of short-statured boreal forest. Common tree species are black spruce (*Picea mariana*), white spruce (*Picea glauca*), Alaska birch (*Betula neoalaskana*), poplar (*Populus* sp.), alder (*Alnus* sp.), and willow (*Salix* sp.), with shrubs dominating the understory. Ground cover includes various moss, sphagnum, lichen, and graminoid species. Dominant forest type varies over relatively small scales (10s to 100s of meters), making the vegetated landscape heterogeneous and complex. The terrain of the YFE is flat, with 95 percent of the area at $\leqslant 3^\circ$ slope as indicated by the National Elevation Dataset. Slopes increase to the south as the region transitions into the White Mountains.

Data

Field Data

A total of 24 field plots were sampled at two sites during the summer of 2010. Each plot represented a 90 m $\times$ 90 m area, with a central transect running nominally north-south through the center of the plot (Figure 2). Three subplots, each 14 m long $\times$ 2 m wide, were centered along the main transect 16 m apart. Vegetation sampling was conducted within these subplots. Diameter at breast height (DBH) and species were recorded for each tree >2 m tall within the subplots. Basal diameter and species were recorded for all trees 1 to 2 m tall and all shrubs >1 m tall. For each 2 m segment along the central transect, within each subplot, the height, height to live crown, and crown radius were measured for the tree (>2 m tall) closest to the segment midpoint. CBD estimates were calculated using the FuelCalc program (Reinhardt *et al.*, 2006), which uses the inventory data (e.g., height, DBH) and a set of species-based allometric equations to calculate plot- or stand-level estimates of CBD. While widely used, FuelCalc is limited by several factors, including a lack of allometric equations for all species and the assumption that vegetation material is distributed evenly within each tree crown. CBD was not estimated for six plots in pure willow, alder, or aspen stands because canopy fire propagation through broadleaf canopies is rare in boreal forests (Van Wagner, 1977).

Airborne Lidar

An airborne lidar survey was conducted in the summer of 2009 for a 2,605 km^2 subarea of the YFE (Figure 1). The data were collected by Aero-Metric, Inc. with an airborne Optec ALTM Gemini and have a horizontal accuracy of 1.15 m, with a nominal point spacing of 2.3 m and a vertical positional accuracy of 0.10 m. The raw data were processed and delivered as bare-earth and first-return digital surface models.

GLAS

The GLAS GLA01 (waveform data) and GLA14 (land/canopy elevation data and footprint locations) products were obtained from the L3f acquisition (release 31) for the entire YFE. The

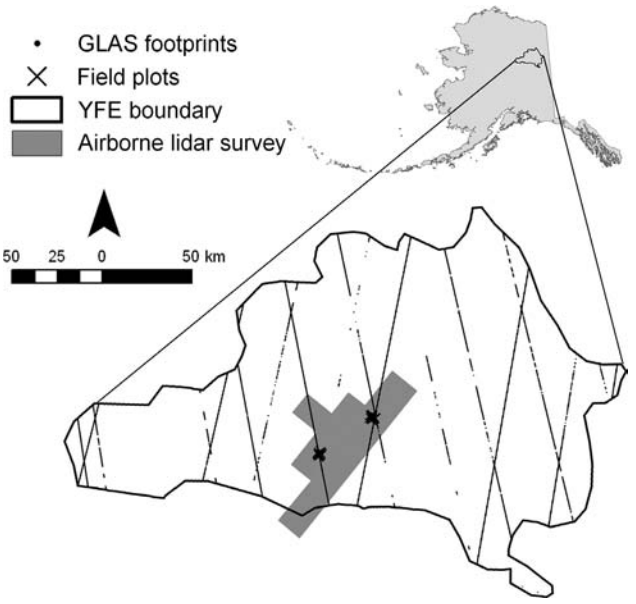

Figure 1. Map of the YFE study area. Extent of the airborne lidar is shown in gray. GLAS footprints for campaign L3f are indicated by the black dots. Field plots are located within the area mapped by the airborne lidar but are not co-located with GLAS footprints.

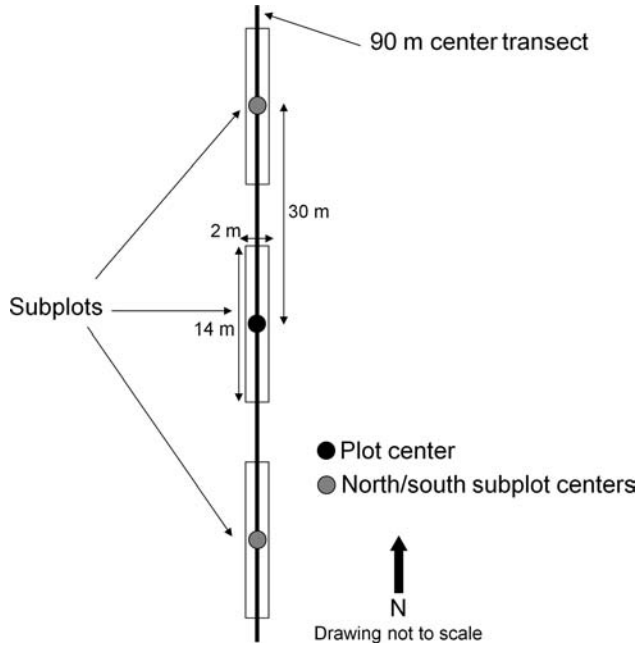

Figure 2. Schematic showing the layout of the central transect and subplots of the field sampling design.

GLA01 product consists of the raw GLAS waveform and statistics about the mean and standard deviation of the background noise. Included in the GLA14 product is a set of metrics describing Gaussian curves fit to the waveform, including number of peaks, width, center, and amplitude of each Gaussian (Harding and Carabajal, 2005). The L3f acquisition occurred between 24 May and 26 June 2006. There are 7,432 GLAS footprints within the YFE study area, with 639 of these falling within the subset area surveyed by the airborne lidar.

Landsat Mosaic

Six Landsat-5 TM scenes acquired between 21 August and 01 September 2008 were converted to at sensor reflectance and brightness temperature. The scenes were mosaicked and clipped to the YFE boundary. Path scene edges were smoothed using a linear regression technique to match adjacent paths (Ji *et al.*, 2012).

Methods

Airborne Lidar

CH, CC, and CBH were derived directly from the lidar point cloud. Height above ground (HAG), representing CH, was derived from the airborne lidar data by differencing the highest first-return value with the mean value of the bare-earth elevation at a 3 × 3 m grid size. A 3 m grid size was chosen because it nested well within the 30 m resolution of the LANDFIRE data, allowed for approximation of most tree crowns, yet still retained substantial vertical information based on the nominal point spacing of the survey (1 point per 2.3 m). Canopy cover was calculated, as defined by McGaughey (2010), as the ratio of lidar returns reflected from above a given height (in this case 3 m), divided by the total number of returns for each 3 m pixel. CBH was estimated by calculating the difference between the lowest non-bare-earth classified return and the bare-earth return per 3 m pixel. If only bare-earth returns were in the 3 m window, the CBH value was zero. While CBH in this case could be understory vegetation and not actual tree branches, the vertical separation of ground and vegetation was the important factor.

CBD is not directly measurable either in the field or from lidar. The methods used to derive CBD are explained in detail in Peterson and Nelson (2011) and are summarized here. For each field plot, the maximum, mean, and minimum HAG values were calculated. Additionally, the lidar point clouds were gridded at 10 m. Within each grid cell the ratio of canopy returns above six height thresholds (at 1 m, 2 m, 3m, 4 m, 5 m, 6 m above ground) to the total number of canopy returns was calculated to provide a measure of changing vertical canopy density. The maximum threshold was set to 6 m because only one plot had a mean HAG height >7 m. From the grid cells intersecting the field plots, the maximum, minimum, and mean of these ratios were calculated to derive plot-level values. These HAG and ratio-derived values were then used as independent variables, while the FuelCalc-based estimates of CBD were used as dependent variables in a stepwise linear regression to identify a model for estimating CBD for all field plots. The model developed in Peterson and Nelson (2011) was then applied to the entire set of airborne lidar data where the National Land Cover Database 2001 Land Cover data (NLCD; Selkowitz and Stehman, 2011) indicated evergreen or mixed forest.

GLAS

Canopy Height

Deriving CH from the GLAS data involved three steps: (a) identifying the signal beginning and signal end in the waveform, (b) identifying the ground and canopy top within the signal, and (c) differencing the canopy top and ground to derive CH (Figure 3). The waveform signal is identified by applying a threshold based on background noise values (Pang *et al.*, 2008). Different noise/signal thresholds were calculated by adding multiples of the background noise standard deviation to the mean background noise values provided in the GLA01 product. Any portion of the waveform above a given threshold value was assumed to be signal. Canopy top was simply inferred as the first return above a given threshold. Because vegetation canopies in the YFE tend to be relatively open and the terrain is very flat, the strongest peak in the waveform can reasonably be assumed to be the ground. Ground was also derived using the method described by Sun *et al.* (2008), for finding the lowest peak within the signal of the waveform. Multiple estimates of CH were calculated for each waveform using combinations of the different noise/signal thresholds and ground finding procedures. Each estimate was compared with the HAG layer, because of a lack of coincident field data. For each GLAS footprint coincident with airborne lidar, a subset area was delineated by a 15 m radius around each footprint center. While the radius of the GLAS footprint is considerably larger, the laser energy is greatest at the footprint center and decreases at further distances, therefore GLAS waveforms are most representative of the footprint centers (Rosette *et al.*, 2010). A circular area with a radius of 15 m around the footprint center encompasses only 12 percent of the footprint area but receives 50 percent of the incident laser energy (Nelson *et al.*, 2009). The maximum HAG value was calculated for each subset, and the CH estimate having the highest correlation with this value was used for further modeling and mapping.

Canopy Cover

CC was estimated from the GLAS waveform following the approach described in Hyde *et al.* (2005), in which the return waveform is separated into ground and canopy energy components, and the relationship between the canopy energy and

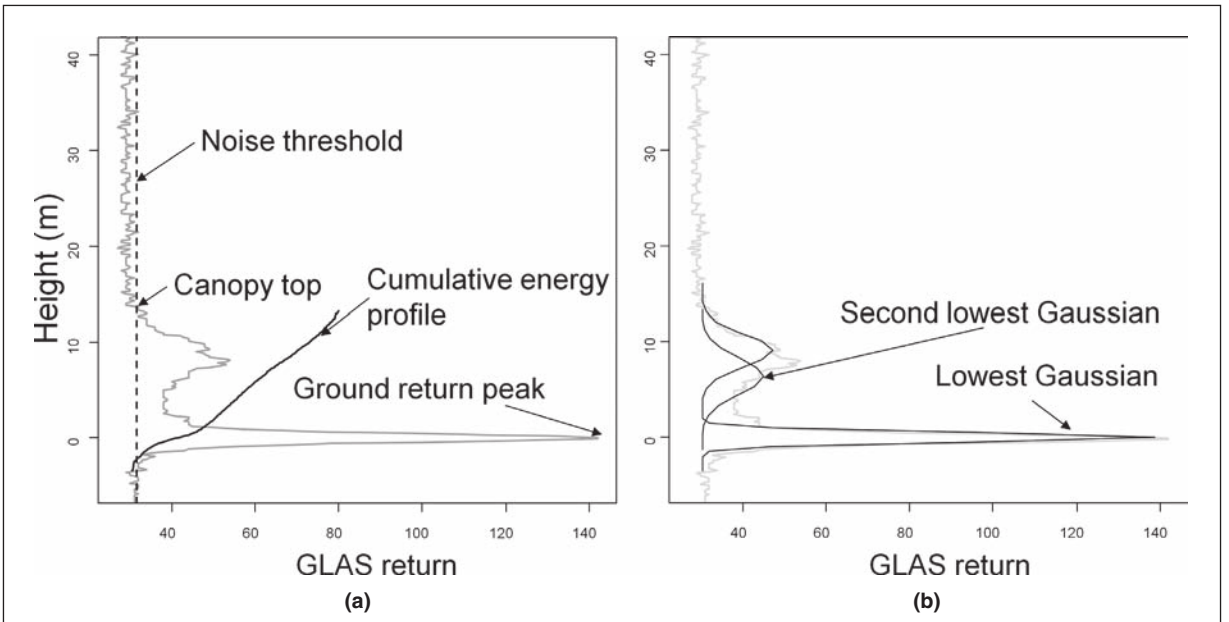

Figure 3. Metrics derived from GLAS waveforms: (a) Example GLAS waveform from the YFE. Canopy top was defined as the first signal above the background noise threshold. The ground was defined as the midpoint of the last waveform peak above the background noise threshold, here the strongest return. The thick black line shows the cumulative energy profile; and (b) Gaussians fit to the waveform. The lowest Gaussian was assumed to correspond to ground, while the second lowest Gaussian was assumed to be influenced by the lower portions of the vegetation canopy.

the total energy of the waveform is assumed to be correlated with CC. Ground cover and other low-lying vegetation can become convolved with the leading edge of the of the ground energy peak, which is otherwise assumed to be symmetrical. Therefore, to obtain a "pure" total ground energy return value, the energy of the trailing half of the ground energy peak, which does not include vegetation signal, was doubled. This ground energy value was subtracted from the total energy in the entire waveform return signal to identify the total canopy energy component. The canopy energy was divided by the total energy resulting in the CC estimate. Hyde *et al.* (2005) adjusted the ground energy value to account for lower reflectance of the ground surface as opposed to vegetation. Here, no adjustment was made to the ground energy total because low, dense ground cover obscured most of the bare ground. As with CH, multiple methods were used to estimate CC using different noise thresholds and ground finding procedures, and the resulting estimates were compared with the airborne lidar CC to select the method used for further mapping.

Canopy Base Height

Two methods were used to identify CBH using GLAS waveform metrics. The first method used the Gaussian metrics identified in the *Data Section* and illustrated in Figure 3. For waveforms delineated by more than one Gaussian, the lowest Gaussian was assumed to be the ground return. The second lowest Gaussian was assumed to be influenced by the vegetation structure of the lower part of the canopy, and therefore, the center and standard deviation values of the second Gaussian were used to derive CBH. A set of metrics was calculated to estimate CBH by multiplying the standard deviation of the second Gaussian by four simple coefficients (0.1, 0.25, 0.5, and 1), and the products were subtracted from the Gaussian center to test which metric was most correlated with CBH derived from the airborne data. The resulting values were used as separate estimates of CBH. In the second method, the 10^{th}, 20^{th}, 30^{th}, 40^{th}, and 50^{th} percentiles of cumulative energy (Figure 3) were used as estimates of CBH. The best method for estimating CBH was identified by comparison with CBH derived from the airborne lidar data.

Canopy Bulk Density

Percentile heights of cumulative waveform energy (Sun *et al.*, 2008), canopy depth, and total waveform energy (Peterson *et al.*, 2007) were derived from the GLAS waveforms. These, plus the Gaussian metrics and GLAS-derived CH, were used as independent variables in a regression analysis. CBD values from the airborne lidar-based map were extracted for each GLAS footprint and used as dependent variables in the regression. A stepwise linear regression procedure was used to identify a model for estimating CBD, which was applied to the rest of the GLAS footprints in the YFE to estimate CBD for those locations.

Extrapolation to YFE

Because the GLAS data are sampled at discrete locations, a regression-tree approach was used to extrapolate GLAS-based CH, CC, CBH, and CBD estimates to the entire YFE by incorporating Landsat TM imagery and ancillary data. Classification and regression trees have been widely utilized for ecological data analysis and classifying remotely sensed imagery because of their ability to model non-linear, complex relationships, yet are relatively simple to implement (De'ath and Fabricius, 2000; Lawrence and Wright, 2001; Yang *et al.*, 2003). The seven Landsat TM spectral bands, elevation, slope, aspect, and NLCD land cover values were used as independent variables. The values for each of these layers were extracted at each GLAS footprint center. For CH, CC, and CBH, the GLAS-derived estimates that were best correlated with the airborne lidar estimates were

used as dependent variables for the modeling and mapping. For CBD, the GLAS metrics utilized in the final regression model were calculated for all waveforms and used to derive CBD which was used as the dependent variable in the regression tree modeling. Cubist (*http://www.rulequest.com*) was used to develop the regression trees, which were then applied to the geospatial datasets to map CH, CC, CBH, and CBD. Cubist is utilized by LANDFIRE, and other projects, for large area mapping because it is an efficient and reasonably accurate tool for generating regression trees (Homer *et al.*, 2012; Reeves *et al.*, 2009). NLCD land cover was used to assign appropriate CBD values to hardwood forest and/or non-forested pixels.

Fire Modeling

To assess the impact of mapping canopy fuel using lidar data, GLAS-derived layers were used to conduct a fire behavior analysis and the resulting outputs were compared with the results using LANDFIRE layers for the same analysis. The FlamMap (Finney, 2006) fire behavior modeling system was used to simulate fire behavior over the YFE. First, FlamMap was run using unmodified LANDFIRE data and averaged weather conditions from a nearby weather station. Then, the four canopy fuel layers were replaced with the GLAS-derived versions and the model was re-run, keeping the rest of the input data and conditions constant. Each FlamMap run produced flame length (FL), rate of spread (ROS), and crown fire activity (CFA) output layers. FL and ROS are continuous outputs measured in meters and meters per minute respectively. The CFA layer separates the landscape into unburned (water, barren, etc.), surface fire only, passive crown fire (individual tree torching), and active crown fire (fire spreading from tree crown to tree crown) classes.

Results

Comparison of Airborne Lidar- and GLAS-derived Fuel Metrics

Canopy Height

Initial comparisons between HAG and GLAS CH resulted in weak correlations, therefore a series of filters were applied to the dataset to strengthen the relationship. Footprints were eliminated that were located on slopes $>3^{\circ}$, were located in non-forested areas (according to NLCD), or had a background noise standard deviation >1.6, resulting in 385 remaining footprints. The correlations improved with the strongest between the maximum HAG value and the GLAS-derived CH estimate using the four standard deviation noise threshold and the maximum peak as the ground location (r = 0.64, root mean square difference (RMSD) = 3.2 m). These parameters were then used to calculate CH for the full set of GLAS waveforms in the YFE, applying the same data filters as above, and the resultant values were used as the dependent variable in the regression tree modeling.

Canopy Cover

Correlations between the airborne lidar-derived and GLAS-derived CC using all 639 footprints were very weak (r <0.1). Applying the same data filters as above, plus eliminating waveforms characterized by a single Gaussian and footprints with <75 percent forest cover according to the NLCD land cover classification, indicating cover type homogeneity, reduced the number of footprints used in the comparison to 152. The strongest relationship was between the maximum airborne lidar-derived CC and the GLAS-derived CC using the 5 standard deviation noise threshold and defining the strongest peak as the ground return (r = 0.61, RMSD = 21.75%). This method for estimating CC was then applied to all of the GLAS waveforms, applying the same data filters listed above, and used as the dependent variable in the regression tree modeling.

Canopy Base Height

Initial comparisons between airborne lidar-derived and GLAS-derived CBH estimates using all 639 footprints showed a very weak relationship (r <0.1). Applying the same filters as for CC above and eliminating footprints where airborne lidar-based CBH estimates were anomalous (<0 and >10 m) reduced the total number of footprints used in the comparison to 31. The strongest relationship was between the maximum airborne lidar-derived CBH value and the 30th percentile cumulative energy GLAS metric (r = 0.50, RMSD = 2.02 m). The 30th percentile height metric was calculated for all GLAS waveforms and, applying the data filters as above, used as the dependent variable in the regression tree modeling.

Canopy Bulk Density

The results of the various modeling steps for CBD can be found in Peterson and Nelson (2011) and are summarized here. The final regression model relating the field data and the airborne lidar metrics had an adjusted R^2 of 0.67, and a residual standard error (RSE) of 0.05 kg m^{-3} and was used to generate the airborne lidar-derived map of CBD. This map was used to obtain the dependent variable for predicting CBD from the GLAS metrics. The best modeling results were obtained after using the same slope, land cover, and single Gaussian filters as above, plus where the standard deviation of the mapped CBD value within a 60 m radius of a footprint center was >0.05 kg m^{-3}. The GLAS footprints were then split into two sets based on NLCD forest class: evergreen forest or mixed evergreen/deciduous forest. The evergreen forest model (N = 30) had an adjusted R^2 of 0.46 and an RSE of 0.03 kg m^{-3}, and the final mixed stands model (N = 29) had an adjusted R^2 of 0.72 and an RSE of 0.06 kg m^{-3}. For the regression tree modeling, all GLAS footprint locations throughout the YFE that passed the filters were separated into forest classes based on NLCD forest type and the appropriate regression model was applied to estimate CBD. These estimates were then used as the dependent variable values in the regression tree modeling.

Comparison of Fuel Maps

CH was binned into two height classes with a break at 10 m to match LANDFIRE. The GLAS-derived CH had 78 percent of pixels mapped in the shorter height class compared to 71 percent of the LANDFIRE pixels. CC was binned into three classes: low (<25 %), medium (≥25 % and <60 %), and high (≥60%). The GLAS-derived CC had 89 percent of pixels mapped in the 25 to 60 percent bin, with 10 percent of pixels in the lowest class and less than 1 percent in the highest class. The LANDFIRE CC had 53 percent of pixels in the middle class with nearly equal amounts in the higher and lower classes. GLAS-derived CBH was slightly lower on average than the LANDFIRE CBH at 1.7 m compared to 2.4 m and had lower variance with standard deviation of 0.9 m and 3.2 m. CBD was higher using GLAS data than LANDFIRE, a trend also observed in the field data.

Fire Modeling Results

Comparing the two FlamMap runs showed a higher incidence of active crown fire using the GLAS-derived canopy fuel layers than when using the LANDFIRE layers, as shown in the CFA output in Figure 4. The area contained in each CFA class using each of the two canopy fuel layers is shown in Table 1. The ROS was higher on average using the LANDFIRE fuel, ranging from 1 to 39 m min^{-1} with a mean of 17, though the range of values was greater using the GLAS-derived canopy fuel, where ROS was between 1 and 85 m min^{-1} with a mean of 14. FL was

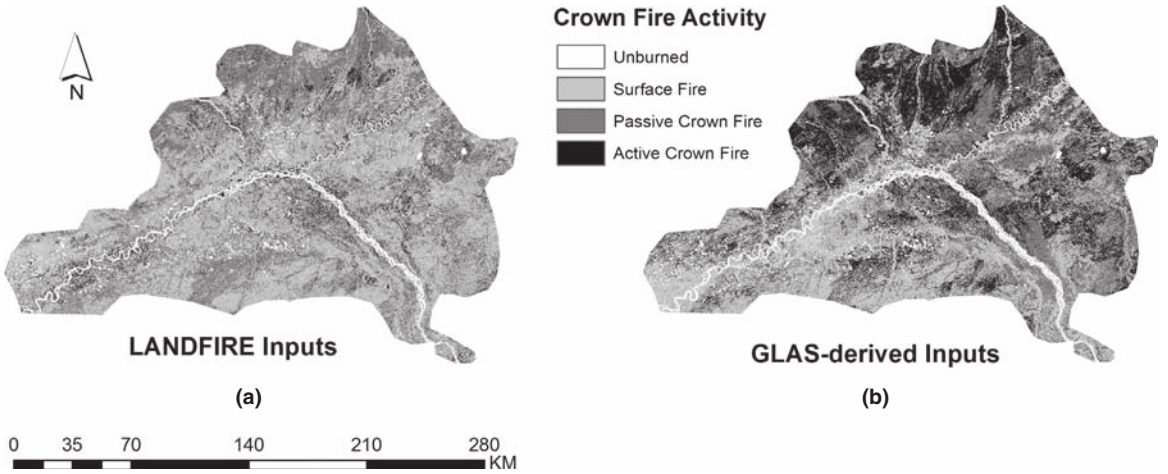

Figure 4. CFA outputs from FlamMap showing the areas that were unburned, and those that burned with surface and crown fires between two runs using (a) LANDFIRE-derived, and (b) GLAS-derived canopy fuel inputs.

lower using LANDFIRE layers, ranging from 1 to 21 m with a mean of 9, compared to 1 to 63 m with a mean of 10 when using the GLAS-derived fuel.

Discussion

Canopy Height

Previous studies have used various characteristics of the GLAS waveform to determine the ground location needed for estimating CH (Lee *et al.*, 2011; Lefsky *et al.*, 2007; Los *et al.*, 2011). This study indicates that for the simple, open structure of the forests in the YFE, the strongest waveform peak appears to be a good indicator of ground. For forests beyond the YFE, this observation will need to be tested, especially in mountainous areas and where denser canopies make detection of the ground more difficult because less energy reaches the ground. The GLAS-derived CH underestimated height relative to the CH derived from the airborne lidar data. This underestimation may be attributed in part to geolocational error and higher HAG values occurring at the fringe of each 15 m radius subset, where illumination energy is lower (Nelson *et al.*, 2009). Furthermore, the GLAS data were collected in the late-spring and early-summer when the vegetation of boreal Alaska is typically not yet full leaf-on, and greater penetration of the lidar energy into the canopy can be expected, in contrast the airborne lidar were collected in mid to late summer. The RMSD of 3.2 m falls within the range reported in previous studies. However, in the short statured forest of boreal Alaska, a 3 m error is significant relative to the total height of the canopy. Even so, incorporating GLAS would provide thematically continuous height estimates, allowing for finer categories than the current LANDFIRE CH layers, and provide height estimates where field data are sparse, resulting in a wider range of ecological and biophysical conditions being represented in the regression tree model.

Table 1. Area Burned by Fire Type Using LANDFIRE- and GLAS-derived Canopy Fuel

	LANDFIRE canopy fuel		GLAS-derived canopy fuel	
Fire Type	Area (ha)	% of burned area	Area (ha)	% of burned area
Surface	1,774,107	57%	1,291,037	42%
Passive Crown	1,018,688	33%	899,202	29%
Active Crown	302,576	10%	908,920	29%

Canopy Cover

As yet, few studies have used GLAS data for deriving CC. Neuenschwander *et al.* (2008) explained 74 percent of the variability between ratios of GLAS canopy to ground energy and percent woody cover estimated from airborne lidar in central Texas. Garcia *et al.* (2012) reported R^2 values of up to 0.89 between GLAS and airborne lidar derived CC estimates using various methods in eastern Texas. In addition, Hyde *et al.* (2005) reported an R^2 of 0.81 between field and LVIS-derived estimates of CC in a Sierra Nevada forest of California. In the present study, the range of CC values from the field data is similar to that predicted from GLAS, indicating that the GLAS estimates are reasonable. The utility of the GLAS-derived CC estimates will need to be explored beyond the flat terrain, open forest conditions of interior Alaska before being applied to other areas. Comparisons with field observed or airborne lidar derived CC in denser forest stands, more mountainous conditions, and/or different surface reflectances will need to be undertaken before using these metrics to inform a national mapping effort. The full range of potential CC values (0 to 100%) would need to be included in an analysis, as both extremely open and closed canopies will pose challenges to the derivation of CC. For mapping large areas, passive optical data such as Landsat imagery are commonly used for estimating CC by applying empirical models (Cohen *et al.*, 2003; Huang *et al.*, 2001).

However, training data are needed to establish meaningful relationships between the Landsat observations and actual CC. The results reported here indicate that GLAS-derived CC could potentially be used as training data for areas lacking field data for modeling. In addition, GLAS data can support mapping CC continuously, rather than large thematic bins as in the LANDFIRE data.

Canopy Base Height

CBH represents a critical canopy characteristic in fire behavior modeling, being a factor in determining the transition from surface to crown fire. However, CBH can be difficult to estimate, and is not directly measurable in the field. Therefore, the ability to consistently estimate CBH using lidar is very appealing. Previous studies using airborne lidar have had varied success in estimating CBH as compared to field-based estimates. Andersen *et al.* (2005) achieved an R^2 of 0.77 deriving plot-level CBH for stands consisting primarily of Douglas-fir (*Pseudotsuga menziesii*) and western hemlock (*Tsuga heterophylla*), in Washington state. Popescu and Zhao (2008) used a tree delineation algorithm to analyze airborne lidar data and predict CBH. R^2 values varied from 0.49 to 0.80 depending on species and lidar characteristics used for the estimation. Vauhkonen (2010) used high density airborne lidar to estimate CBH with R^2 values ranging between 0.71 to 0.84 depending on lidar metrics used for model building. Peterson *et al.* (2007) used LVIS data to estimate CBH for a Sierra Nevadan forest, with an R^2 of 0.59. The use of GLAS data for deriving CBH, as presented here, is novel. To achieve a meaningful relationship between the airborne lidar- and GLAS-based CBH estimates, severe filtering of the GLAS data was required. However, the volume of GLAS data available over large areas allows such filtering while still leaves sufficient footprints to use for modeling.

A particular challenge to deriving CBH from waveform lidar data is separating low vegetation from the ground return. The strong ground signals commonly observed in the GLAS waveforms for the YFE make this somewhat easier. This will become more difficult in areas of steeper terrain as the ground pulse spreads and in denser canopy areas as the ground pulse is weakened. The percentiles of waveform energy were better indicators of CBH than the Gaussian-based estimators, indicating that these might be more sensitive to the bulk density threshold needed to carry fire from the surface into the canopy. However, as underscored by the strict filtering needed to obtain meaningful correlations between the GLAS and airborne lidar derived CBH estimates; this work is still exploratory. Better field data representing the lower portion of the canopy and understory vegetation and co-located with GLAS footprints would allow a better examination of how the waveform shape relates to the canopy structure and, therefore, better demarcation of the CBH threshold in the waveform.

Canopy Bulk Density

The regression model relating the airborne lidar and field-based CBD explains nearly 70 percent of the variability in the data set. This is lower than those reported by Andersen *et al.* (2005; $R^2 = 0.84$) and Erdody and Moskal (2010; $R^2 = 0.83$). The results reported by Riaño *et al.* (2004) varied considerably depending on which method was used to identify lidar canopy returns and the regression equation used to predict CBD (R^2 up to 0.80). Several factors likely affected these results: (a) the FuelCalc CBD allometries were not available for some boreal species, (b) the field data are not representative of the full range of CBD values present within the YFE, and (c) the dominant vegetation type in the YFE changes across relatively small spatial scales (10s to 100s of meters), leading to within-plot variability. The studies listed above conducted their work using data collected in relatively homogenous plots, which simplifies both the calculation of field-based CBD and the derivation of lidar metrics.

The results of the GLAS-based CBD prediction are comparable to previous work by Peterson *et al.* (2007) using LVIS data to derive CBD in the mixed conifer forests of the Sierra Nevada, who reported an R^2 of 0.71. Garćia *et al.* (2012) derived CBD from GLAS data in forested areas of eastern Texas, reporting an R^2 of 0.78. In the present study, splitting the GLAS footprints by forest type resulted in an R^2 of 0. 61 for evergreen forests and an R^2 of 0.72 for mixed forests. This split likely resulted in a stronger relationship between the GLAS-based estimates of CBD and the field-based estimates because CBD was not calculated for hardwood species. Therefore, two waveforms may be described by similar metrics, but one falling in an evergreen stand will have a much higher CBD associated with it than one falling into a mixed stand with a large percentage of hardwoods.

Comparisons of Canopy Fuel Maps

A formal accuracy assessment of the canopy fuel maps is not available at this time due to lack of available field data. However, other studies have found common limitations of the LANDFIRE canopy fuel layers including CBH and CC values being too high, and CBD values being too low (e.g., Krasnow *et al.*, 2009). As shown in the results, these issues appear to be mitigated in the GLAS-derived layers. LANDFIRE field data in many parts of Alaska were very sparse, especially for structural data. Additionally, much of the available structural data were collected through aerial surveys and classified into broad classes rather than continuous estimates of forest height and canopy cover. These broad classes obscure much of the spatial variability present on the landscape. LANDFIRE maps of CBH and CBD also relied on expert opinion of expected fire behavior under historic weather conditions, with the canopy fuel values modified to reflect the expert's approximations. The GLAS-based canopy fuel maps, with the exception of CBD, are also not directly related to field observations. However, because lidar is inherently sensitive to vegetation structure, there is high confidence in the estimates derived from lidar and, consequently, the maps extrapolated from these estimates. Moreover, because of the spatial distribution of GLAS footprints throughout the YFE, the study area is well represented by GLAS data, so more of the spatial variability of the landscape is captured in the canopy fuel maps.

FlamMap Modeling

The outputs of the FlamMap modeling analyses indicate significant differences between the model runs using different sources of canopy fuel data. Many of the differences can be attributed to the thematic resolution of the canopy fuel layers. Specifically, the continuous fuel layers derived from GLAS capture more of the spatial detail of the landscape than the binned LANDFIRE layers, and therefore the FlamMap outputs show much more spatial detail as well. It is not possible to validate the actual values of the fire behavior model outputs for a given pixel, because the model runs were entirely theoretical, based on historical but arbitrary weather conditions. However, significant differences existed between model runs and the spatial patterns in the output tended to better represent the features on the landscape using the GLAS-derived canopy fuel. This leads to the conclusion that the GLAS-derived fuel layers enable a more detailed fire behavior analysis and that the current operational fire behavior modeling systems are sensitive to the more detailed canopy fuel information. The outputs of these models are used for both strategic planning and tactical incident response to make resource management decisions with significant impacts to communities, ecosystems, and agency budgets. Therefore, it is advantageous to incorporate the best available data and methods into developing the inputs for fire models, to ensure the best resource management decision making. The availability of nationwide, consistent, three-dimensional geospatial data will allow future canopy fuel data to be more detailed and higher quality than those available using imagery alone.

Conclusions

Currently, GLAS is integral to any regional or national lidar-based mapping of vegetation canopy structure as it represents the only data set consistently available at those scales. Multiple applications require consistent nationwide three-dimensional canopy data. As more studies demonstrate the utility of GLAS data for vegetation structure derivation over a variety of forest and topographic conditions it becomes apparent that programs such as LANDFIRE will greatly benefit from including these data. The decommissioning of GLAS in 2010 has presented a challenge to continuing these large-area lidar assessments of canopy structure required by LANDFIRE and similar programs. While a follow-on mission is expected to be launched in the near future, it is still important for users of such data to continue to foster the creation of a comprehensive, high-quality national three-dimensional lidar dataset suitable for landscape mapping. For large portions of the nation, high quality data regarding forest structure continue to be sparse; yet such data are becoming more essential to the characterization of fire behavior and the informing of other resource management objectives.

Acknowledgments

This work was supported by LANDFIRE, the USGS Climate Effects Network, and the USGS Climate & Landuse Change Research and Development Program. The authors wish to thank Dana Nossov, Mark Winterstein, Neal Pastick, Jason Stoker, Lei Ji, and Karl Heidemann for assistance with data collection and processing. Dr. Peterson's work was performed under USGS contract number G08PC91508. The use of any trade, product, or firm name is for descriptive purposes only and does not imply endorsement by the US Government.

References

Andersen, H.-E., R.J. Mcgaughey, and S.E. Reutebuch, 2005. Estimating forest canopy fuel parameters using LIDAR data, *Remote Sensing of Environment*, 94(4):441–449.

Cohen, W.B., T.K. Maiersperger, S.T. Gower, and D.P. Turner, 2003. An improved strategy for regression of biophysical variables and Landsat ETM+ data, *Remote Sensing of Environment*, 84(4):561–571.

De'ath, G., and K.E. Fabricius, 2000. Classification and regression trees: A powerful yet simple technique for ecological data analysis, *Ecology*, 81(11):3178–3192.

Drake, J.B., R.O. Dubayah, D.B. Clark, R.G. Knox, J.B. Blair, M.A. Hofton, R.L. Chazdon, J.F. Weishampel, and S. Prince, 2002. Estimation of tropical forest structural characteristics using large-footprint lidar, *Remote Sensing of Environment*, 79(2-3):305–319.

Dubayah, R.O., and J.B. Drake, 2000. Lidar remote sensing for forestry, *Journal of Forestry*, 98(6):44–52.

Erdody, T.L., and L.M. Moskal, 2010. Fusion of LiDAR and imagery for estimating forest canopy fuels, *Remote Sensing of Environment*, 114(4):725–737.

Falkowski, M.J., P.E. Gessler, P. Morgan, A.T. Hudak, and A.M.S. Smith, 2005. Characterizing and mapping forest fire fuels using ASTER imagery and gradient modeling, *Forest Ecology and Management*, 217(2-3):129–146.

Finney, M.A., 2006. An overview of FlamMap fire modeling capabilities, *Proceedings of Fuels Management - How to Measure Success*, 28–30 March, Portland, Oregon (US Department of Agriculture, Forest Service, Rocky Mountain Research Station, Proceedings RMRS-P-41, Fort Collins, Colorado), pp. 213–220.

Gallant, A.L., E.F. Binnian, J.M. Omernik, and M.B. Shasby, 1995. *Ecoregions of Alaska*, US Geological Survey, Professional Paper 1567, Washington, D.C., pp. 78.

García, M., S. Popescu, D. Riaño, K. Zhao, A. Neuenschwander, M. Agca, and E. Chuvieco, 2012. Characterization of canopy fuels using ICESat/GLAS data, *Remote Sensing of Environment*, 123(1):81–89.

Harding, D.J., and C.C. Carabajal, 2005. ICESat waveform measurements of within-footprint topographic relief and vegetation vertical structure, *Geophysical Research Letters*, 32(21):L21S10.

Homer, C.G., C.L. Aldridge, D.K. Meyer, and S.J. Schell, 2012. Multi-scale remote sensing sagebrush characterization with regression trees over Wyoming, USA: Laying a foundation for monitoring, *International Journal of Applied Earth Observation and Geoinformation*, 14(1):233–244.

Huang, C., L. Yang, B.K. Wylie, and C.G. Homer, 2001. A strategy for estimating tree canopy density using Landsat 7 ETM+ and high resolution images over large areas, *Proceedings of the 3rd International Conference on Geospatial Information in Agriculture and Forestry*, 05-07 November, Denver, Colorado, unpaginated CD-ROM.

Hyde, P., R. Dubayah, B. Peterson, J. Blair, M. Hofton, C. Hunsaker, R. Knox, and W. Walker, 2005. Mapping forest structure for wildlife habitat analysis using waveform lidar: Validation of montane ecosystems, *Remote Sensing of Environment*, 96(3-4):427–437.

Ji, L., B.K. Wylie, D.R. Nossov, B. Peterson, M.P. Waldrop, J.W. Mcfarland, J. Rover, and T.N. Hollingsworth, 2012. Estimating aboveground biomass in interior Alaska with Landsat data and field measurements, *International Journal of Applied Earth Observation and Geoinformation*, 18(1):451–461.

Keane, R.E., S.A. Mincemoyer, K.M. Schmidt, D.G. Long, and J.L. Garner, 2000. *Mapping Vegetation and Fuels for Fire Management on the Gila National Forest Complex, New Mexico*, US Department of Agriculture, Forest Service, Rocky Mountain Research Station, General Technical Report RMRS-GTR-46, Ogden, Utah, pp. 126.

Krasnow, K., T. Schoennagel, and T.T. Veblen, 2009. Forest fuel mapping and evaluation of LANDFIRE fuel maps in Boulder County, Colorado, USA, *Forest Ecology and Management*, 257(7):1603–1612.

Lawrence, R.L., and A. Wright, 2001. Rule-based classification systems using classification and regression tree (CART) analysis, *Photogrammetric Engineering & Remote Sensing*, 67(10): 1137–1142.

Lee, S., W. Ni-Meister, W. Yang, and Q. Chen, 2011. Physically based vertical vegetation structure retrieval from ICESat data: Validation using LVIS in White Mountain National Forest, New Hampshire, USA, *Remote Sensing of Environment*, 115(11):2776–2785.

Lefsky, M.A., W.B. Cohen, G.G. Parker, and D.J. Harding, 2002. Lidar remote sensing for ecosystem studies, *BioScience*, 52(1):19–30.

Lefsky, M.A., M. Keller, Y. Pang, P.B. De Camargo, and M.O. Hunter, 2007. Revised method for forest canopy height estimation from Geoscience Laser Altimeter System waveforms, *Journal of Applied Remote Sensing*, 1(1):013537.

Los, S.O., J.a.B. Rosette, N. Kljun, P.R.J. North, J.C. Suárez, C. Hopkinson, R.A. Hill, L. Chasmer, E. Van Gorsel, C. Mahoney, and J.a.J. Berni, 2011. Vegetation height products between 60 deg S and 60 deg N from ICESat GLAS data, *Geoscientific Model Development Discussions*, 4(3):2327–2363.

Mcgaughey, R.J., 2010. *Fusion/LDV: Software for LiDAR data analysis and visualization*, US Department of Agriculture, Forest Service, Pacific Northwest Research Station, pp. 166.

Morsdorf, F., E. Meier, B. Kötz, K.I. Itten, M. Dobbertin, and B. Allgöwer, 2004. LIDAR-based geometric reconstruction of boreal type forest stands at single tree level for forest and wildland fire management, *Remote Sensing of Environment*, 92(3): 353–362.

Nelson, R., K.J. Ranson, G. Sun, D.S. Kimes, V. Kharuk, and P. Montesano, 2009. Estimating Siberian timber volume using MODIS and ICESat/GLAS, *Remote Sensing of Environment*, 113(3):691–701.

Neuenschwander, A.L., T.J. Urban, R. Gutierrez, and B.E. Schutz, 2008. Characterization of ICESat/GLAS waveforms over terrestrial ecosystems: Implications for vegetation mapping, *Journal of Geophysical Research*, 113(G2):G02S03.

Pang, Y., M. Lefsky, H.-E. Andersen, M.E. Miller, and K. Sherrill, 2008. Validation of the ICEsat vegetation product using crown-area-weighted mean height derived using crown delineation with discrete return lidar data, *Canadian Journal of Remote Sensing*, 34(SUPPL. 2):S471–S484.

Peterson, B., R. Dubayah, P. Hyde, M. Hofton, J.B. Blair, and J. Kaufman, 2007. Use of lidar for forest inventory and management application, *Proceedings of the Seventh Annual Forest Inventory and Analysis Symposium*, 03-06 October 2005, Portland, Maine (US Department of Agriculture, Forest Service, Washington Office, General Technical Report WO-77, Washington, D.C.), pp. 193–200.

Peterson, B., and K. Nelson, 2011. Developing a regional canopy fuels assessment strategy using multi-scale lidar, *Proceedings of Silvilaser 2011*, 16-20 October, Hobart, Tasmania, pp. 8.

Popescu, S.C., and K. Zhao, 2008. A voxel-based lidar method for estimating crown base height for deciduous and pine trees, *Remote Sensing of Environment*, 112(3):767–781.

Reeves, M.C., K.C. Ryan, M.G. Rollins, and T.G. Thompson, 2009. Spatial fuel data products of the LANDFIRE Project, *International Journal of Wildland Fire*, 18(3):250–267.

Reinhardt, E., D. Lutes, and J. Scott, 2006. FuelCalc: A method for estimating fuel characteristics, *Proceedings of Fuels Management - How to Measure Success*, 28–30 March 2008, Portland, Oregon (US. Department of Agriculture, Forest Service, Rocky Mountain Research Station, Proceedings RMRS P-41, Fort Collins, Colorado), pp. 273–282.

Riaño, D., E. Chuvieco, S. Condés, J. González-Matesanz, and S.L. Ustin, 2004. Generation of crown bulk density for Pinus sylvestris L. from lidar, *Remote Sensing of Environment*, 92(3):345–352.

Rollins, M.G., R.E. Keane, and R.A. Parsons, 2004. Mapping fuels and fire regimes using remote sensing, ecosystem simulation, and gradient modeling, *Ecological Applications*, 14(1):75–95.

Rollins, M.G., 2009. LANDFIRE: A nationally consistent vegetation, wildland fire, and fuel assessment, *International Journal of Wildland Fire*, 18(3):235–249.

Rosette, J.a.B., P.R.J. North, J.C. Suárez, and S.O. Los, 2010. Uncertainty within satellite LiDAR estimations of vegetation and topography, *International Journal of Remote Sensing*, 31(5):1325–1342.

Selkowitz, D.J., and S.V. Stehman, 2011. Thematic accuracy of the National Land Cover Database (NLCD) 2001 land cover for Alaska, *Remote Sensing of Environment*, 115(6):1401–1407.

Selkowitz, D.J., G. Green, B. Peterson, and B. Wylie, 2012. A multisensor lidar, multi-spectral and multi-angular approach for mapping canopy height in boreal forest regions, *Remote Sensing of Environment*, 121(1):458–471.

Sun, G., K.J. Ranson, D.S. Kimes, J.B. Blair, and K. Kovacs, 2008. Forest vertical structure from GLAS: An evaluation using LVIS and SRTM data, *Remote Sensing of Environment*, 112(1): 107–117.

Van Wagner, C.E., 1977. Conditions for the start and spread of crown fire, *Canadian Journal of Forest Research*, 7(1):23–34.

Vauhkonen, J., 2010. Estimating crown base height for Scots pine by means of the 3D geometry of airborne laser scanning data, *International Journal of Remote Sensing*, 31(5):1213–1226.

Yang, L., C. Huang, C.G. Homer, B.K. Wylie, and M.J. Coan, 2003. An approach for mapping large-area impervious surfaces: synergistic use of Landsat-7 ETM+ and high spatial resolution imagery, *Canadian Journal of Remote Sensing*, 29(2):230–240.